Available online at www.worldscientificnews.com

World Scientific News

An International Scientific Journal

WSN 201 (2025) 195-221 EISSN 2392-2192

Chemically Modified Groundnut Shell Adsorbent: A Mean To Removing Peroxide (PO), Free Fatty Acid (FFA), and Acid (ACD) from Used Vegetable Oil

Abidemi Anthony Sangoremi[1], Oluwayemi Olanike E. Onawumi[2], Olugbenga Solomon Bello[2]

[1]Department of Chemistry, Federal University Otuoke, PMB 126, Yenagoa, Bayelsa State, Nigeria

[2]Department of Pure and Applied Chemistry, Ladoke Akintola University of Technology, Ogbomoso, Oyo State, Nigeria

Correspondent author: Email address: sangoremiaa@fuotuoke.edu.ng

ABSTRACT

Responsiveness on the adverse effects of various toxic constituents of used vegetable oil (UVO) with its adverse consequences on man's health such as cancer and cardiovascular diseases gave rise to the challenge of recovering UVO for reuse. Hence, this research investigated the potentials of groundnut shell activated carbon (GSAC) on the recovery of UVO. The biosorbent was analysed for physicochemical parameters, in addition to Fourier transform infrared spectrometer (FTIR), Scanning electron micrograph, electron dispersive X-ray spectroscope analysis. Batch adsorption technique was employed, and operational parameters like contact time, dosage and temperature were studied. Adsorption data were subjected to isotherm and kinetic models. The adsorbent showed high fixed carbon contents and surface area, FTIR revealed various functional groups which are potential adsorption sites, and SEM showed a well-developed pore structure. The EDX established the presence of elements such as oxygen, calcium, and carbon in the percentage composition. The percentage recovery efficiency (% R) on PV, FFA and AV from UVO at optimum conditions (12g, 80 min, 60 ºC) was: (87.11, 79.14, 84.00 %), (86.75, 79.28, 84.00 %) and (72.41, 79.13, 80.24 %) respectively. The peroxide (PO) and free fatty acid (FFA) adsorption were best fitted by Freundlich isotherm model, while the acid (ACD) removal was best described by Brouers Weron Sotolongo-Coasta (BWS) isotherm model. On the other hand, PO and FFA removal were best described by BWS kinetic model, while ACD was best fitted for pseudo-second-order (PSO) kinetic model.

(Received 10 January 2025; Accepted 20 February 2025; Date of Publication 11 March 2025)

Additionally, the adsorption process was thermodynamically feasible at the temperature range studied with the negative values of Gibbs free energy (-ΔG), positive value of enthalpy change (+ΔH), and negative values of entropy change (-ΔS). Conclusively, GSAC stands an efficient, promising, and eco-friendly adsorbent for UVO regeneration, as it improves the quality of the oil to near virgin.

Keywords: Contact time, FTIR, kinetic models, isotherm models, thermodynamics. Corresponding authors Emails: sangoremiaa@gmail.com

1. INTRODUCTION

Generation and disposal of waste have been a major concern globally and many studies have validated these assertions [1-7]. Most of these wastes are generated from different sources, such as agriculture, food processing, electrical, chemical, domestic, brewing, paper, oil and gas to mention just a few. Regenerating, recovering, recycling these wastes to useful material would be of huge benefit to man, his environment and generate income to the society at large [8, 9]. Agrowastes had been utilized effectively in contemporary waste treatment [10]. Agro-wastes had been exploited efficaciously in current polluted soil remediation [11-17], effluent/wastewater treatment [18,19], adsorption of pesticide [20], waste oil adsorption [21] dye adsorption [22-24], removal of heavy metal from aqueous solutions [25], purification of used vegetable oil [27], removal of Malachite Green dye [28], sugarcane bagasse in recovery of used sunflower oil [29, 30] and circumvention against novel Corona virus (SARS CoV 2) [31]. Commercially available activated charcoals are costly because of their utilization of non-sustainable and generally significant expensive starting materials, for example, coal which are not appropriate regarding ecological contamination control measure [32]. Used vegetable oils (UVO) is used broadly in modern and homegrown food handling, with deep fried food items being one of its essential applications. Food frying is a prevalent foods preparation method [33]. Deep frying oil is a practice of dipping food in hot oil with a interaction amid oil and oxygen at elevated temperature (150-190^{o}C) [34, 35]. UVO could be regenerated to become suitable for reuse. The remediation procedure includes the removal of colour, odour, FFA, PO, ACD from UVO [36-37]. These regeneration procedures might incorporate bleaching, synthetic balance, concentration and deodourization [38]. Large numbers of recovery routes have deficiencies such as cost including fragmented evacuation of impurities in UVO. The use of chemical to remove impurities from UVO may not be wellthought-out as a green route, hence, the need for a suitable, green and clean process [39].

Groundnut shell (GS) is an agricultural post-harvest waste of leguminous plant. Technically, groundnut, also known as *Arachis hypogaea*, has dry pericarp. The shells are the dry pericarp containing cellulose, carbohydrate, protein, minerals and lipids [40].

2. MATERIALS AND METHODS

2.1. Materials

1a 1b

Plate 1. Agro-wastes
a. Groundnut shell b. Pulverized groundnut shell

2.2. Samples Procurement, Preparation, and Modification

GS samples were obtained from homestead, Idi-Osan, Boripe LGA, Osun State, Nigeria. It was washed carefully with regular water from the research facility and cleaned adequately with distilled water to eliminate dust and debris. GS samples were oven-dried for 5 hours at 105ºC after sun dried for 24 hours, cooled in desiccators and pulverized to a chosen particle size [8]. The technique described by [33] was used by using 0.3 M orthophosphoric acid (H_3PO_4). A cautiously weighed 14.0 g GS samples were placed in 250 ml Erlenmeyer flask having 0.3 M H_3PO4. The contents of the flask were carefully heated and mixed on a hot plate pending the formation of a paste. The paste of GS samples was placed in a crucible and put in a furnace at 500 ºC for 60 minutes. Subsequently, the samples were permitted to cool and wash severally with deionized water to a pH of 7.10. Thereafter, the biosorbent was kept in a sealed glass bottle for usage.

2.3. Preparation of Used Vegetable Oil

5-litres king vegetable oil was procured at a native marketplace in Osogbo, Nigeria. The manufacturing and expiry dates were ascertained. The oil was divided into portion and labeled. The first portion was the vegetable oil that was not used, the second portion was used in frying iced fish ten times. The peroxide value (PO), free fatty acid (FFA) and acid value (ACD) were determined from all the portions.

2.4. Quality Parameters Analysis in Vegetable Oil

2.4.1. Peroxide Value

The peroxide value (PV) was determined by dissolving 5 g of the sample in 30 cm^3 of glacial acetic acid: chloroform (3:2 v/v) then 0.5 cm^3 of potassium iodide was added. The solution was titrated with standard sodium thiosulphate using starch indicator. Peroxide value was calculated using the equation [8].

$$(1) \qquad PV\,(m_{eq}O_2/kg) = \frac{S - BxMx1000}{W}$$

B and S are titre values of blank and sample respectively, W is the sample weight, M is the molarity of $Na_2S_2O_3$

2.4.2. Acid Value

Acid value (AV) was determined by using the method by Onawumi *et al*. (2017). The oil sample (1.0g) was boiled with 50 cm^3 neutral ethanol, then it was allowed to cool, and 2 drops of phenolphthalein indicator were added. The resulting solution was titrated against 0.1N KOH until a pink colour was obtained. The acid value was calculated using the formula [8]:

$$(2) \qquad AV\,(mgKOH/g) = \frac{VxNx56.1}{W}$$

V is the titre value, Normality of KOH, and W is the weight of oil, 56.1 molecular weight of KOH **2.4.2. Free fatty acid value**

The oil sample (10g) was taken into a clean and dry conical flask, to which 25 ml neutralized 95 % ethanol was added and well mixed to dissolve the oil in ethanol. Phenolphthalein was added as an indicator. Content of flask was titrated against KOH solution, Shaking constantly until a pink colour persisted for 30 minutes. The percentage of free fatty acid (FFA) was calculated as [8].

$$(3) \qquad FFA(\%) = \frac{VxNx28.2}{W}$$

V is the titre value, N is the normality of KOH, and W is the weight of oil sample.

2.5. Batch Adsorption Process

The batch adsorption technique was adopted at varying conditions. The methods used by [8] for UFVO were employed. The oil samples were mixed with mixture of dried powdered groundnut shell activated carbon (GSAC) at ratio of 100 ml: 4 g (v/w). Oil and adsorbents were mixed using magnetic stirrer and heated for 20 minutes at 30°C. The biosorbent was separated from the oil by filtration of hot suspension on Buchner's funnel with filter paper in a vacuum (10-15 mm Hg) for 2 hours. The cool filtrates were stored in sealed bottle for further analysis. A number of experimental variables such as adsorbent dosage in the range of (4-20 g), contact time (20-100 min) and temperature (30-70 °C) were studied. The adsorbed quantity of oil parameters at equilibrium, q_e (mg/g) was calculated by the expression:

$$(4) \qquad q_e = \frac{(Co - Ce)*V}{M}$$

Where Co, Ce (mg/L); M (g) and V (L) are: initial, equilibrium concentrations, mass of adsorbent used, and volume of oil samples in liter respectively. The percentage impurities removal was determined as follows:

$$(5) \qquad \%R = \frac{(Co - Ce)}{C_o} *100$$

2.5.1. Adsorbent Dosage Studies

Different dosages of groundnut shell activated Carbon (GSAC); 4, 8, 12, 16, 20 g were weighed and added to 100 ml UVO put into Erlenmeyer flasks at optimum conditions. Oil and adsorbents were mixed using magnetic stirrer and heated, while keeping the time and temperature constant.

The biosorbent was removed from the oil by filtration of hot suspension on Buchner's funnel with filter paper in a vacuum (10-15 mm Hg) for 2 hours. The cool filtrates were stored in sealed bottles for further analysis [8].

2.5.2. Contact Time Studies

The effects of contact time on the abstraction of PO, FFA, and ACD from UVO onto GSAC was investigated by varying the time in the range of 20-100 min, while keeping the dosage and temperature constant.

2.5.3. Temperature Studies

Adsorbents were added to UVO and agitated at 30, 40, 50, 60, 70 °C until equilibrium was attained while other factors remain the same. The process was carried out in triplicate.

2.6. Software Application on Adsorption Models

In order to enhance the design, the plan framework for the abstraction of adsorbates, it is essential to lay out the most fitting connection for the adsorption equilibrium curves. KyPlot, version 2.00 software was employed. Coefficient of determination (R^2), normalized Chi-square error (χ^2) and sum square of error (SSE) were utilized to decide the model that best depicted the equilibrium data of the different biosorbents [41]. The numerical conditions for χ^2 and SSE [42] are: Normalized Chi-square error test,

$$x^2 = \sum_{K=1}^{N} \left| \frac{(q_{k,\exp} - q_{k,pred})^2}{(q_{k,pred} - q_e)^2} \right| \quad (6)$$

Ne

Coefficient of determination

$$R^2 = 1 - \frac{\sum_{k=1}^{Ne} (q_{k,\exp} - q_{k,pred})^2}{\sum_{k=1} (q_{k,pred} - q_e)^2} \quad (7)$$

2.7. Isotherm Models and Their Nonlinear Equations

Brouers Weron Sotolongo (BWS), $q_e = q_{\max}(1(\exp(-K_w C_e^{\square})$ (8)

Freundlich, $q_e = K_F C_e^{1/n}$ (9)

Jovanovich, $q_e = q_m(1 - e^{KJ} C_e)$ (10)

Langmuir, $q_e = \frac{K^L q^m C^e}{1 + K\,LCe}$ (11)

Sips, $q_e = 1 + a_s \frac{k^s C^e \square_s \square}{Ce}$ (12)

2.8. Kinetic Models Nonlinear Equations

BWS, $q_t = q_e(1 - ne^{\square})$ (13)

Fractal pseudo-second order (FPSO), $q_t = 1 + K_f q_e t_a$ (14)

Pseudo-first-order (PFO), $q_t = q_e(1 - e^{-k_1 t})$ (15)

Pseudo-second-order (PSO), $q_t = \frac{k_2 q_{e2} t}{1 + k_2 q_e t}$ (16)

3. RESULTS AND DISCUSSION

3.1. Characterization of GSAC

3.1.1. Physicochemical Properties

Table 1 presented the physicochemical analysis carried out on the biomass. The pH, moistness content (MC), vaporizable material (VM), bulk density (BD), ash content (AC), and bound carbon (FC) were within the range of those found in literature [3, 8]. The prepared GSAC possesses high fixed carbon content and surface area (SA) that boost good adsorption. A good activated carbon should possess a SA of 500-1500 m^2/g [43].

Table 1. Physicochemical properties/composition of modified groundnut shell adsorbent (GSAC)[8].

S.No	Parameter	Mean ± SE
1	Moisture substance (%)	14.10 ± 0.101
2	pH	7.10 ± 0.101
3	Fixed carbon (%)	67.70 ± 0.010
4	Particle size (µm)	300 ± 0.000
5	Ash substance (%)	8.98 ± 0.111
6	Volatile matter (%)	9.20 ± 0.112
7	Surface area (m^2/g)	880.00 ± 0.100
8	Bulk thickness (g/cm3)	0.508 ± 0.000

3.1.2. FTIR Analysis

The exterior functional groups determination by FTIR for biosorbent is revealed in Figure 1. The FTIR spectral of GSAC show certain adsorption peaks that are indicative of functional groups. The spectra indicate that the adsorbent has potential adsorption site as represented by the functional groups like: OH, C-C, C-N, and COOH which influence the surface chemistry of GSAC. The band at 3533.71 cm^{-1} is ascribed to non-bounded OH stretch, the signal at 3286.61 cm^{-1} proposed OH stretching of carboxylic acid, while the signal at 1635.69 cm^{-1} suggested the N-H of amine and amide, the band at 1442.80 cm^{-1} showed that of C-C and $–CH_3$, and the peak at 987.59 is attributed to C-C functional group. Other authors got similar results [3, 8, 41].

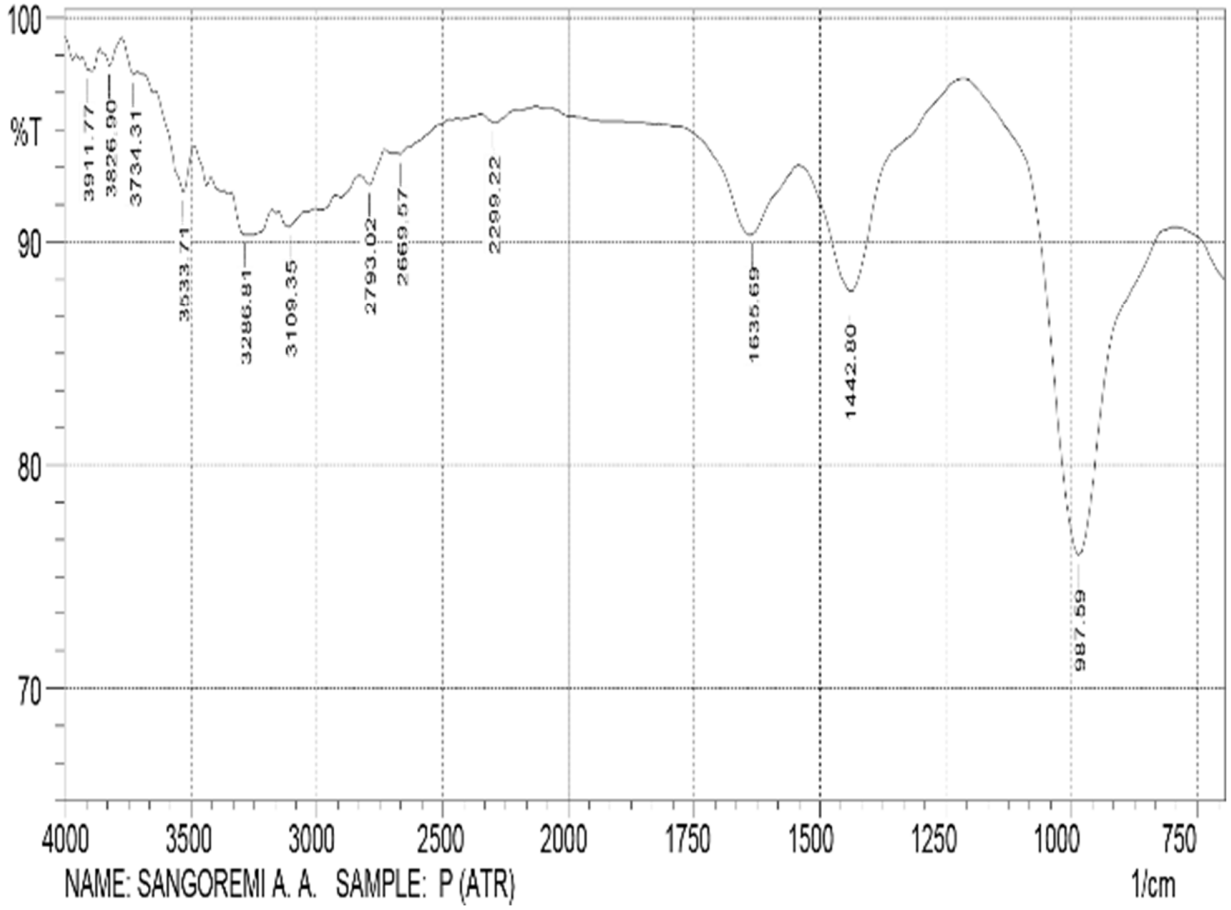

Figure 1. FTIR spectral analysis of GSAC

3.1.3. SEM/EDX Analysis

Figure 2 reveals the scanning electron micrograph (SEM) of GSAC. The surface morphology revealed that the volatiles were released within the microstructure, and after acid treatment with H_3PO_4, several pores were formed as seen in the micrograph. This is an evidence that activation of biosorbent with orthophosphoric acid promotes better porosity, high carbon content, and improved surface reactivity. In addition, the presence of element like carbon, oxygen, silicon, calcium, magnesium, and aluminum in percentage weights was revealed by EDX (Figure 3) [35].

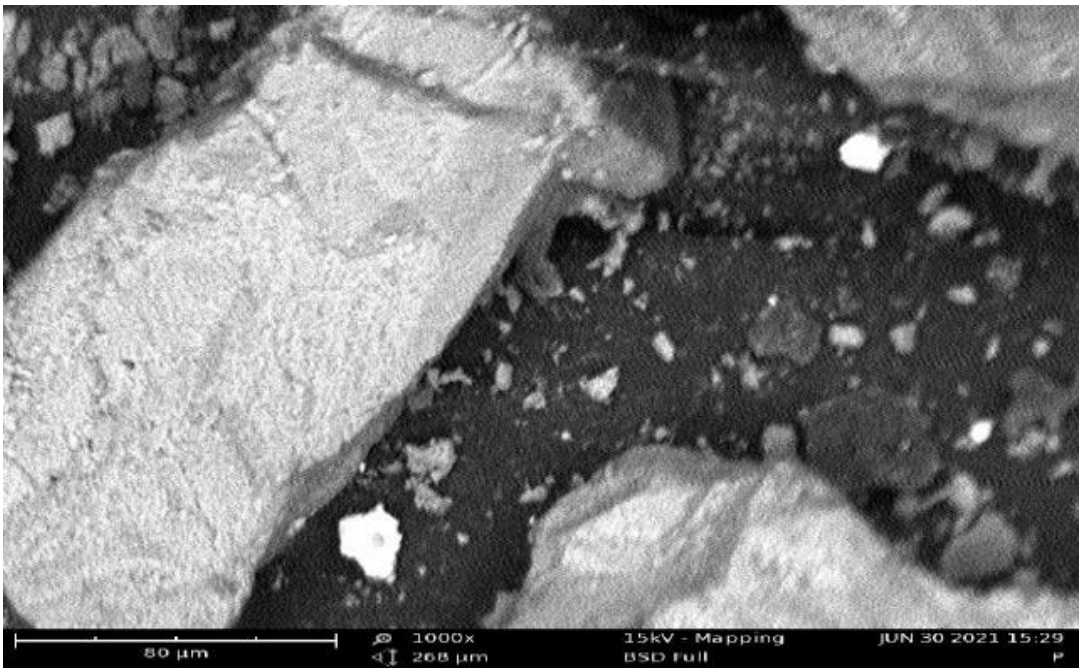

Figure. 2 SEM analysis of GSAC

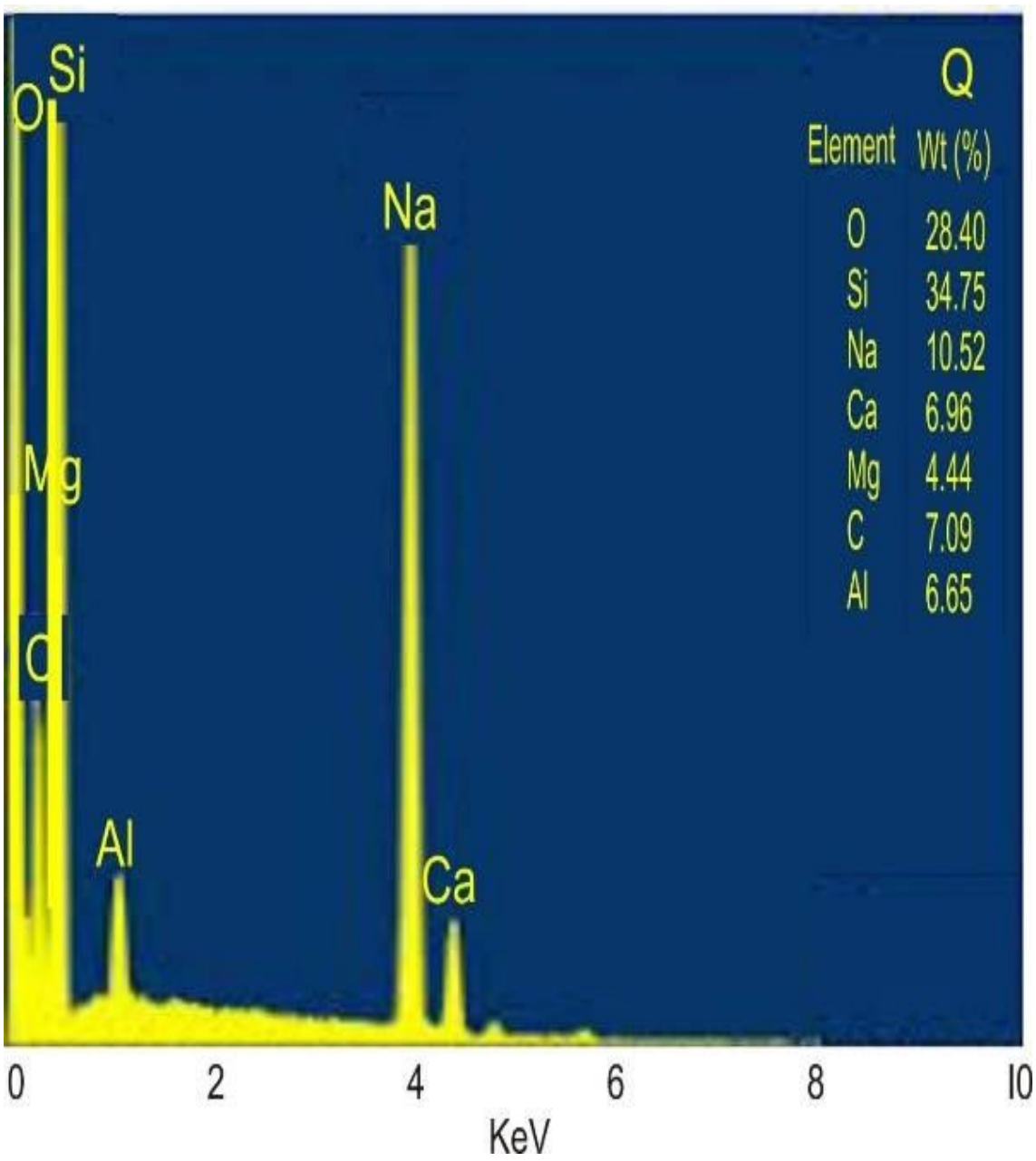

Figure 3. EDX spectra analysis of GSAC

3.2. Effects of Working Parameters

3.2.1. Effects of Biosorbent Dosage

The dependence of percentage removal (% R) of PO, FFA and ACD on the amount of GSAC is represented in Figure 4. It was observed that the recovery efficiency of PO, FFA and ACD from UVO improved with a rise in biosorbent dosage. The opinion could be ascribed to the accessibility of extra sites and increasing pore surface areas. This further encourages easier penetration of PO, FFA and ACD molecules from UVO onto the GSAC adsorption sites. [42] made similar observations in their work when FFA was removed from waste cooking oil (WCO). In the current study, the maximum % adsorption at optimum conditions was (87.11, 79.14, 84.00 %) of PO, FFA and ACD respectively.

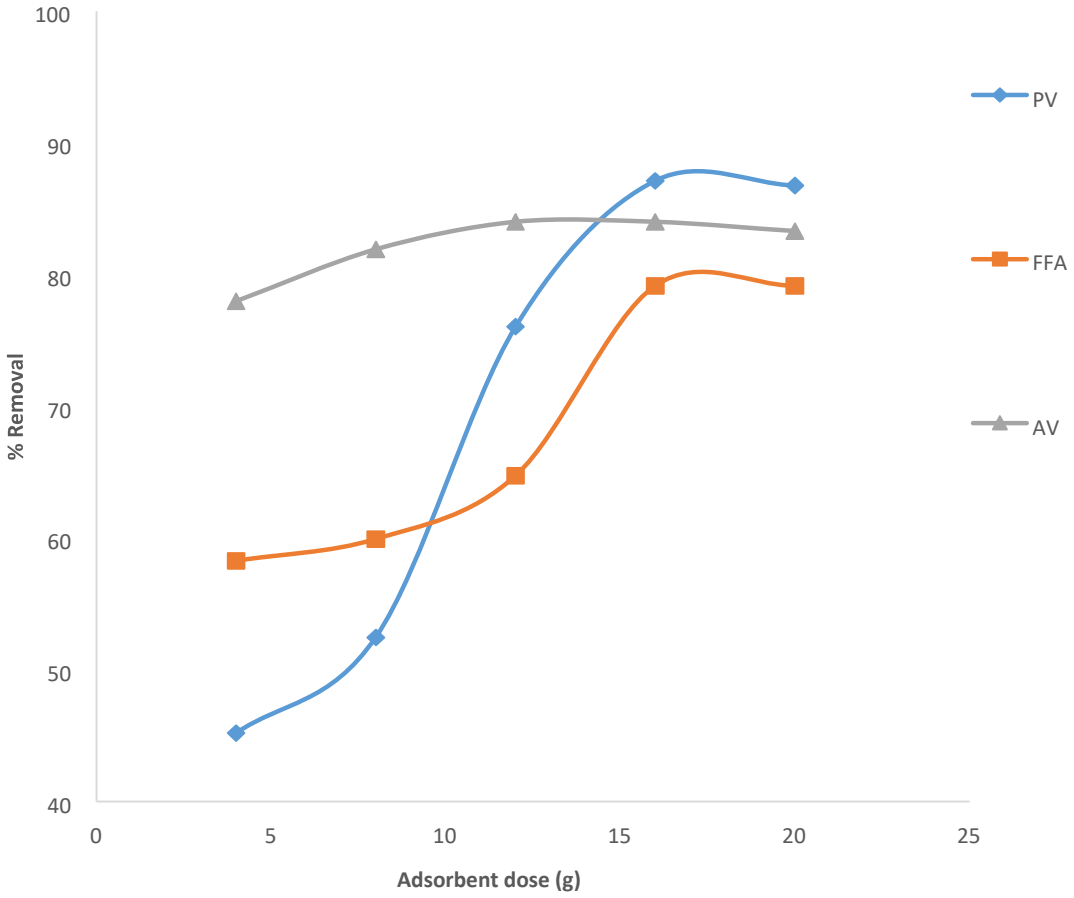

Figure 4. Plots of adsorbent dosage on PO, FFA & ACD removal onto GSAC.

3.2.2. Effects of Contact Time (CT)

The impacts of contact time on the abstraction of PO, FFA and ACd was studied by changing the contact time in the range of 20-100 minutes while keeping the dosage and temperature constant. Figure 5 shows the connection between the contact time and percent bond (% bond). The % bond increased with increasing contact time until equilibrium was established [44]. With further increase in time from 80 to 100 minutes, % bond marginally increase and/or reduced as more sites are being occupied until equilibrium was reached when adsorption sites were fully saturated or there were no free molecules of PO, FFA or ACD in UVO. This is termed adsorption-desorption phenomenon [45]. The optimum % bond was (86.75, 79.28, 84.00 %) for PO, FFA and ACD, respectively. This was in agreement with the results of other researchers [43].

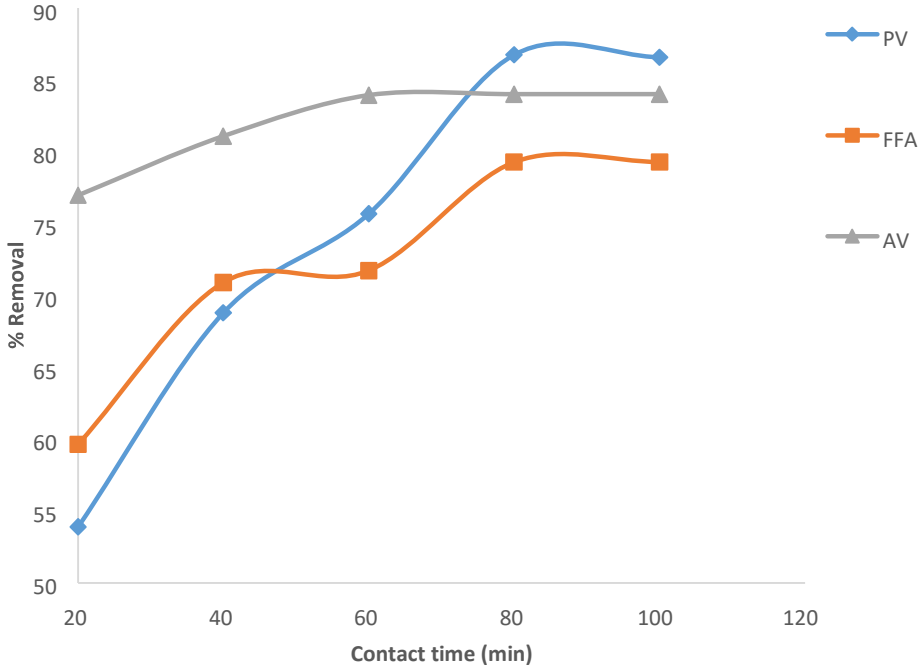

Figure 5. Plots of Contact Time on PO, FFA & ACD abstraction onto GSAC.

3.2.3. Effects of Temperature

The relationship between the temperature and percentage removal (% R) are presented in Figure 6. The % R of PO, FFA and ACD increased as temperature increases from 30 to 70 ºC. This may be due to expansion in portability of the molecules as kinetic energy increases with increasing temperature in addition to the swelling of adsorbent pores which allow penetration of more molecules. The optimum % R of PO, FFA and ACD from UFVO was (72.41, 79.13, 80.24) in that order.

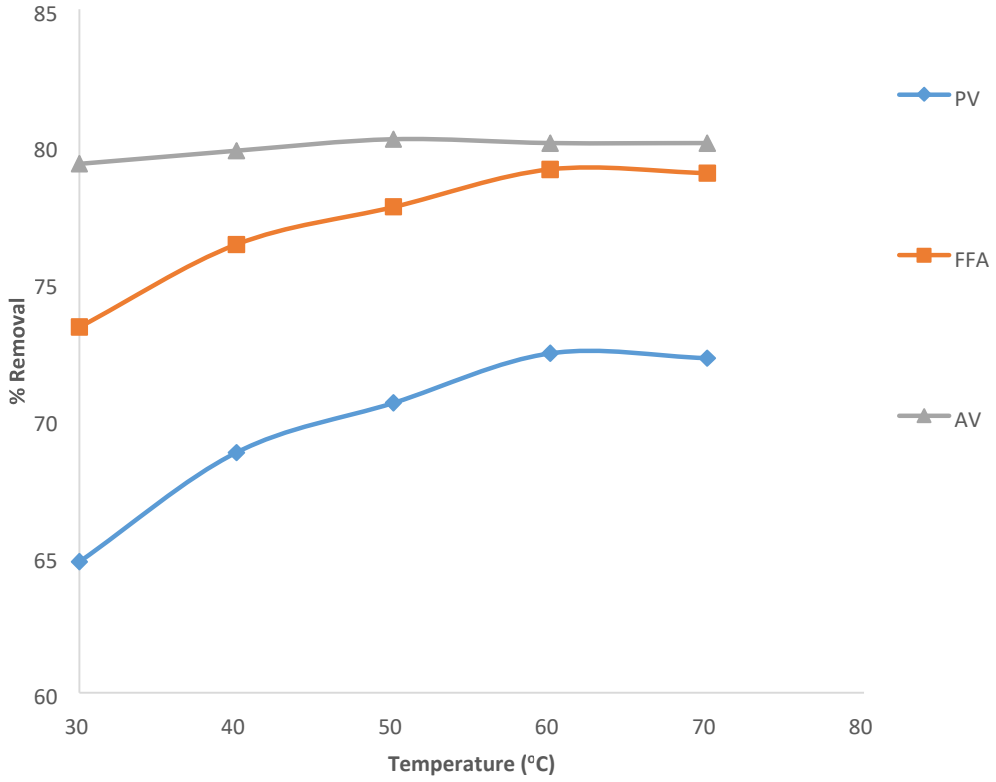

Figure 6. Plots of temperature on PO, FFA & ACD removal onto GSAC.

3.2.4. Effects of Working Parameters and Adsorption Capacity

Figures 7, 8 and 9 showed the effects of dosage, contact time, and temperature on the adsorption capacity respectively. The maximum adsorption capacity and GSAC dosage on PO, FFA, and ACD was 6.23×10^{-2} $LM_{eq}O_2 1000^{-1}$, 1.06×10^{-1} mgL and 2.87×10^{-1} mgL respectively. Observation was made that the adsorption capacity of the biosorbent toward PO, FFA and ACD got reduced as dosage increased. This perception might be because of an inadequate mass transfer of adsorbate over the adsorbent as the dosage increases. Contrariwise, increase in contact time leads to increasing adsorption capacity, while temperature increase marginally increased with increase in temperature, this may be due to effective mass transfer of the adsorbate over the adsorbent as contact time and temperature increases.

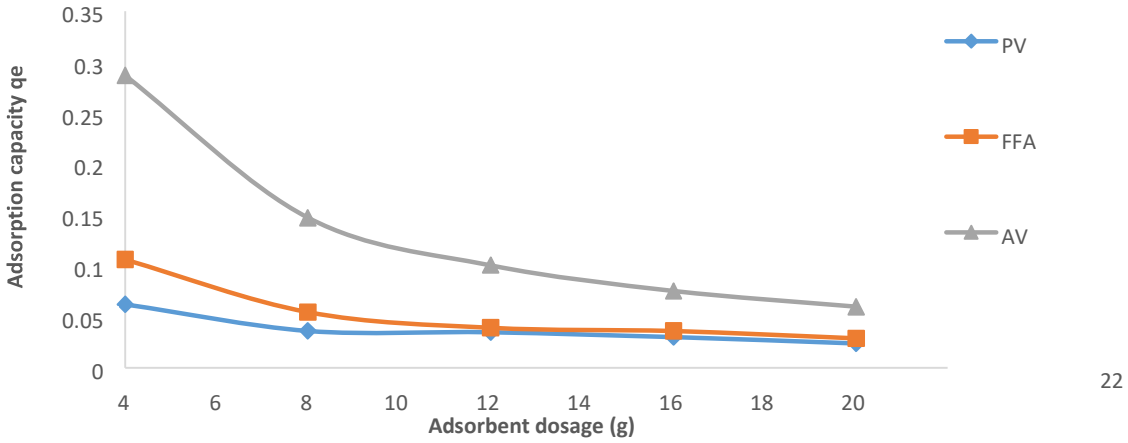

22

Figure 7. Relationship between dosage and adsorption capacity.

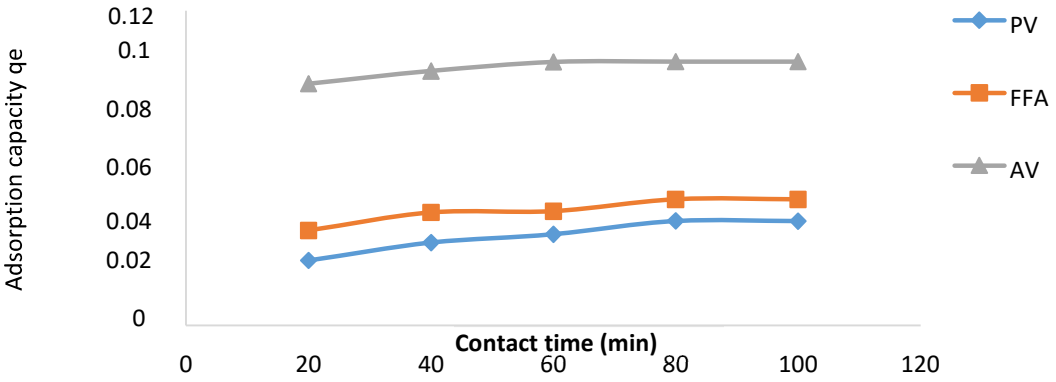

Figure 8. Relationship between contact time and adsorption capacity.

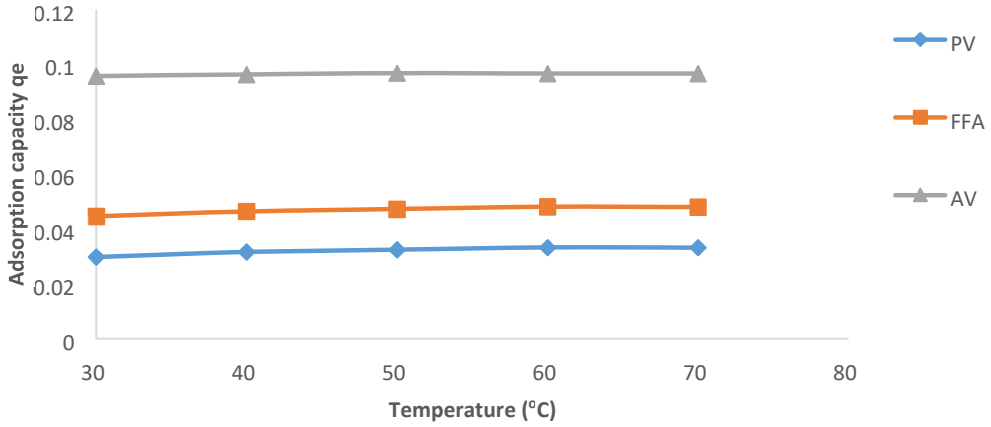

Figure 9. Relationship between temperature and adsorption capacity.

3.3. Adsorption Mechanisms

3.3.1. Adsorption Equilibrium Studies

The experimental data were subjected to isotherm data using non-linear equations by employing KyPlot® version 2.0 software. Isotherm models used include Brouers Weron Sotolongo-Coasta (BWS), Freundlich, Jovanovich, Langmuir and Sips. The coefficient of determination, normalized chi-square error, and sum of square errors were employed to estimate the goodness of fit. Figure 10a, c and e indicate the isotherm model of PO, FFA, and ACD onto GSAC, and Table 2 shows the isotherm parameters. The Table 2 revealed that Freundlich model was the only model that mostly and best modelled the PO, FFA and ACD from UFVO onto GSAC with coefficient of determination

(R^2 = 0.8611, 0.7326 and 0.9606), normalized chi-square error (χ^2) (7.05E-005, 4 x 10^{-3} and 5.0 x 10^{-4}), sum of square error SSE (3.0 x 10^{-3}, 1.7 x 10^{-3}, 1.9 x 10^{-3}) respectively. Since Freundlich model best describes the goodness of fit, it then suggests that the adsorption is more of physiosorption and multilayer on heterogeneous surface. Also, the closeness of the coefficient of determination to unity and low error values signify goodness of fit [43].

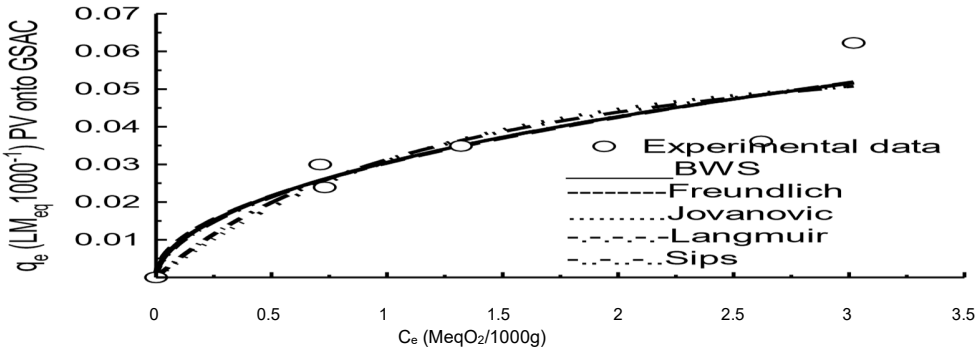

Figure 10a. Adsorption isotherm model plots of PO onto GSAC.

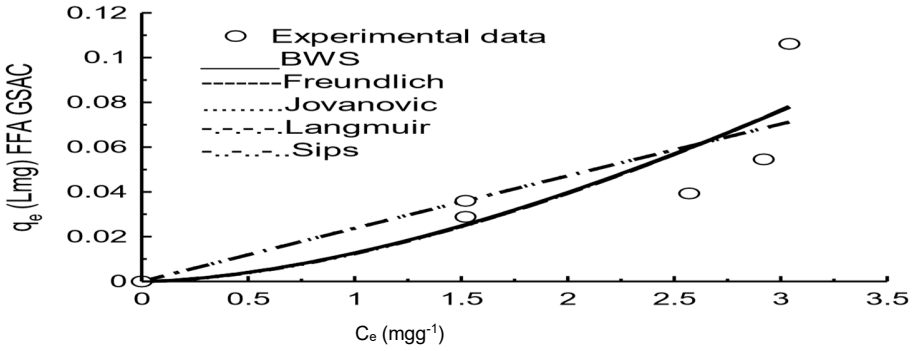

Figure10b. Adsorption isotherm model plots of FFA onto GSAC.

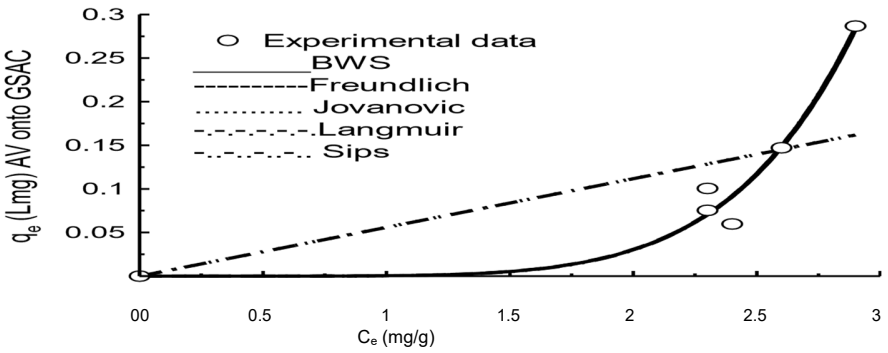

Figure 10c. Adsorption kinetic model plots of ACD onto GSAC.

Table 2. Adsorption Isotherm Parameters of PO, FFA and ACD onto GSAC

PO, FFA & ACD Isotherm model	**Adsorbents**	**GSAC**		
BWS	Parameters	PO	FFA	ACD
	q_{max} (mg/g)	0.1739	0.7680	5.6253
	n	0.1932	0.0167	7.96E-005
	K_w	0.5433	1.6686	6.0862
	R^2	0.8591	0.7304	0.9604
	R	0.9269	0.8546	0.9800
	x^2	9.53E-005	0.0006	0.0006
	SSE	0.0003	0.0017	0.0019
Freundlich				
	K_F	0.0304	0.0126	0.0005
	n	2.0606	0.6102	0.1668
	R^2	0.8611	0.7326	0.9606
	R	0.9279	0.8559	0.9801
	x^2	7.05E-005	0.0004	0.0005
	SSE	0.0003	0.0017	0.0019
Jovanovic				
	q_{max} (mg/g)	0.0555	1.3700	30.9074
	K_J (g/mg/min)	0.8177	0.0175	0.0018
	R^2	0.8368	0.6926	0.4910
	R	0.9148	0.8322	0.7007
	x^2	8.28E-005	0.0005	0.0062
	SSE	0.0003	0.0019	0.0247
Langmuir				
	q_{max}	0.0734	3.6931	61.0596
	K_L	0.7429	0.0065	0.0009
	R^2	0.8464	0.6935	0.4910
	R	0.9200	0.8327	0.7007
	x^2	7.8E-005	0.0005	0.0062
	SSE	0.0003	0.0019	0.0247
Sips				
	q_{max} (mg/g)	0.2446	1.3828	5.0931
	a_s(g/mg/min	0.0333	0.0627	0.2185
	Ks	0.5732	1.6998	6.1963
	R^2	0.8586	0.7303	0.9601
	R	0.9266	0.8546	0.9799
	x^2	9.57E-005	0.0006	0.0006
	SSE	0.0003	0.0017	0.0019

3.3.2. Adsorption kinetic studies

The experimental data were subjected to four kinetic models which are Brouers Weron SotolongoCoasta (BWS), Fractal pseudo-second order (FPSO), Pseudo-first-order (PFO) and Pseudo-second order (PSO). Figures 11a, b and c respectively show the kinetic models of PO, FFA and ACD onto GSAC and Table 3 revealed the kinetic parameters of PO, FFA and ACD adsorption. The Table 3 indicated that BWS kinetic model best fitted the PO adsorption, PSO possess the goodness of fit for FFA while PSO and FPSO best described the ACD adsorption with the following coefficient of determination (R^2 = 0.9970, 0.9970, 0.998 = 0.998), normalized chi square error (χ^2) (1.11E-006, 1.84E-006 and 1.17E-006), sum of square error SSE (3.34E-006, 5.52E-006, 4.67E-006) respectively. Since BWS gave the goodness of fit for PO, it connotes that the time taken to adsorb half of the equilibrium quantity is probable. The PSO of FFA and FPSO on ACD suggested that the procedure was second-order rate controlled and the adsorption is more of chemisorption.

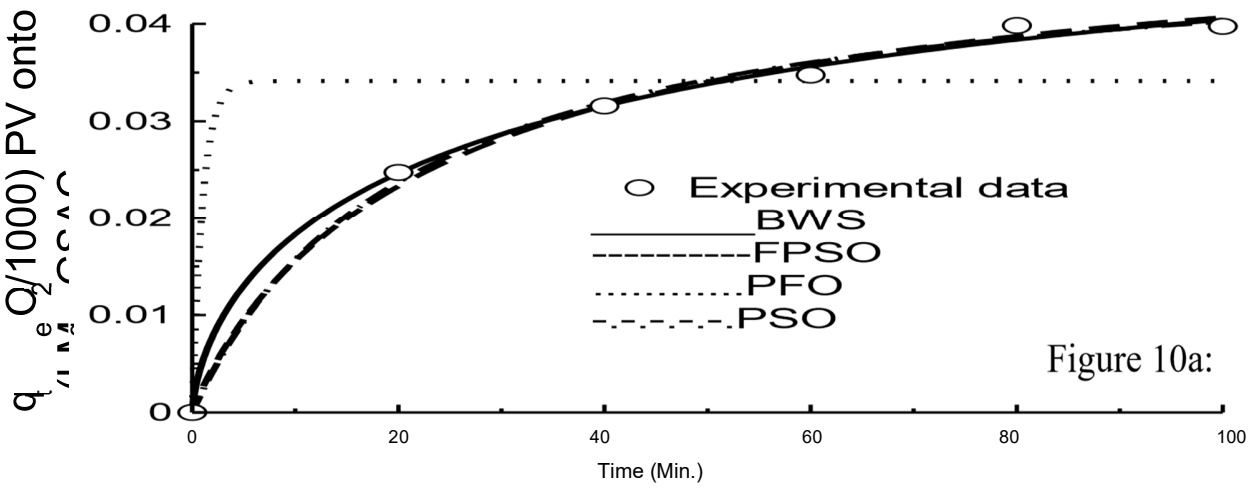

Figure 11a. Adsorption kinetic model plots of PO onto GSAC.

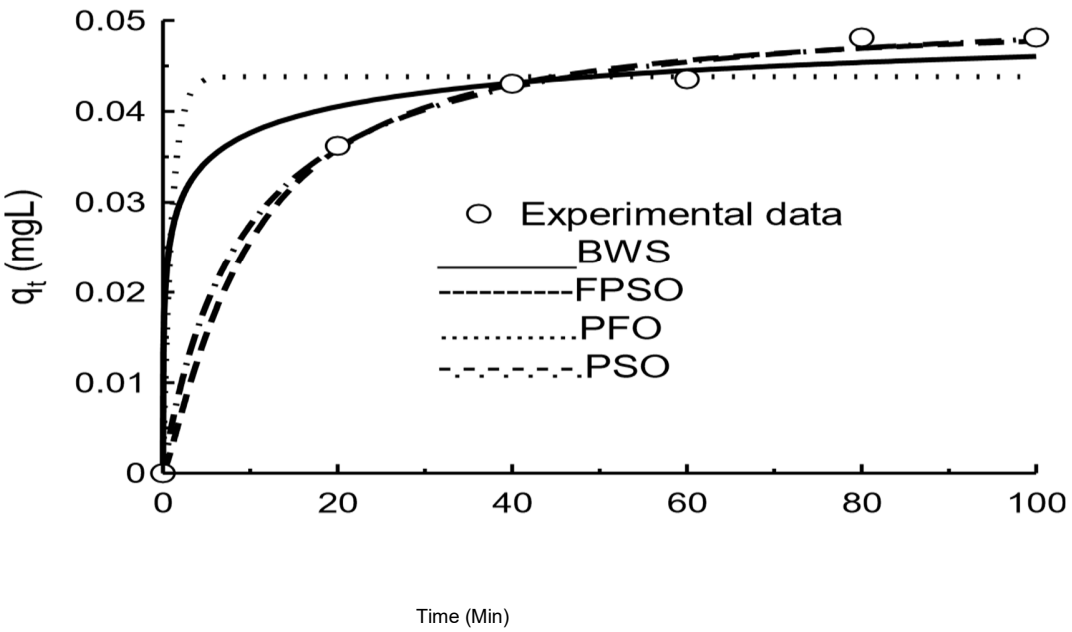

Figure 11b. Adsorption kinetic model plots of FFA onto GSAC.

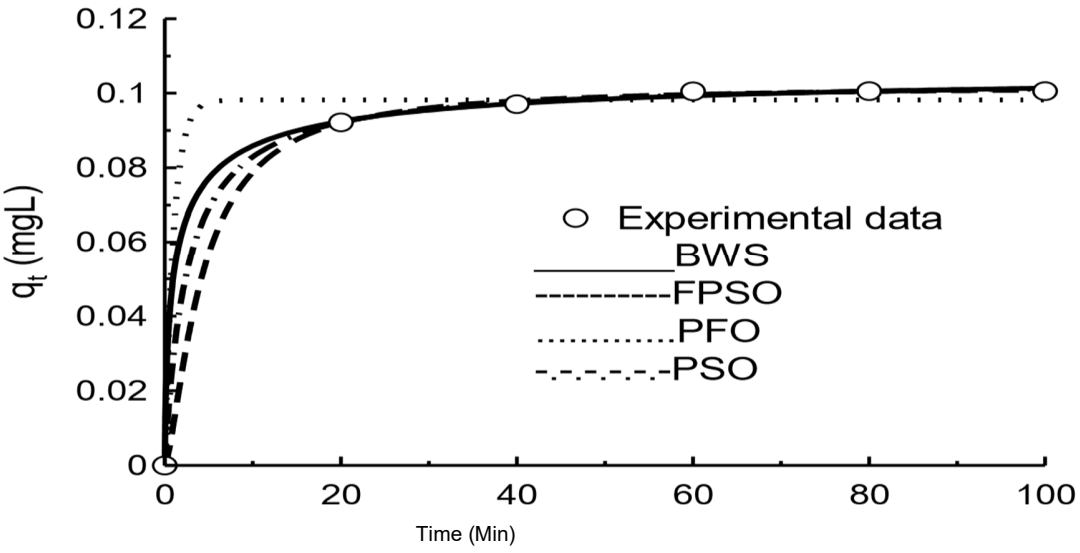

Figure 11c. Adsorption kinetic model plots of ACD onto GSAC.

Table 3. Adsorption Kinetic Parameters of PO, FFA and ACD onto GSAC.

PO Kinetic model	**Adsorbent**			
BWS	Parameters	PO	FFA	ACD
	q_e(mg/g)	0.0610	0.0559	0.1070
	n	0.0279	0.7609	0.8707
	A	0.6606	0.3554	0.6493
	R^2	0.9970	0.9815	0.9997
	R	0.9985	0.9907	0.9999
	x^2	1.11E-006	1.0E-005	7.19E-006
	SSE	3.34E-006	3.13E-005	2.16E-005
FPO				
	q_e (mg/g)	0.9806	1.1828	1.2302
	K_F	0.0518	0.0504	0.1019
	t^a	0.9284	1.2422	1.4346
	R^2	0.9951	0.9964	0.9998
	R	0.9976	0.9982	0.9999
	x^2	1.84E-006	2.01E-006	5.39E-007
	SSE	5.52E-006	6.03E-006	1.62E-006
PFO				
	q_e (mg/g)	0.0341	0.0438	0.0982
	K_1 (g/mg/min)	1.0000	1.0000	1.0000
	R^2	0.8593	0.9436	0.9933
	R	0.9270	0.9714	0.9966
	x^2	3.97E-005	2.39E-005	1.36E-005
	SSE	0.0002	9.57E-005	5.43E-005
PSO				
	q_e (mg/g)	0.9810	2.1255	3.8590
	K_2 (g/mg/min	0.0486	0.0523	0.1037
	R^2	0.9959	0.9970	0.9998
	R	0.9979	0.9985	0.9999
	x^2	1.17E-006	1.29E-006	3.77E-007
	SSE	4.67E-006	5.14E-006	1.51E-006

3.3.3. Thermodynamic Studies

The thermodynamic studies of PO, FFA and ACD adsorption onto GSAC emerged with varying outcomes as presented in Table 4. The plots of ln Kc against 1/T is presented in Figure 12 at temperature ranged of 303 to 343 K. The adsorption of PO, FFA and ACD onto the adsorbent studied, the Gibbs free energy change (ΔG) has negative values (-4.78 x 10^3 to -4.40 x 10^3, -4.28 x 10^{3-} to -3.94 x 10^3, -4.61 x 10^4 to -4.99 x 10^3 kJmol^{-1}). The adverse values of ΔG showed that the procedure was extemporaneous and thus established the feasibility of the adsorption process
(Jabar *et al*., 2022). The positive value of enthalpy change (ΔH) (7.59 x 10^4, 6.84 x 10^4, 1.72 x 10^4 kJmol^{-1}) proposed that the adsorption process was endothermic and the negative values of entropy change (ΔS) suggested that the adsorption was well-ordered signifying a suitable conformation of PO, FFA and ACD on the exterior of GSAC [46]

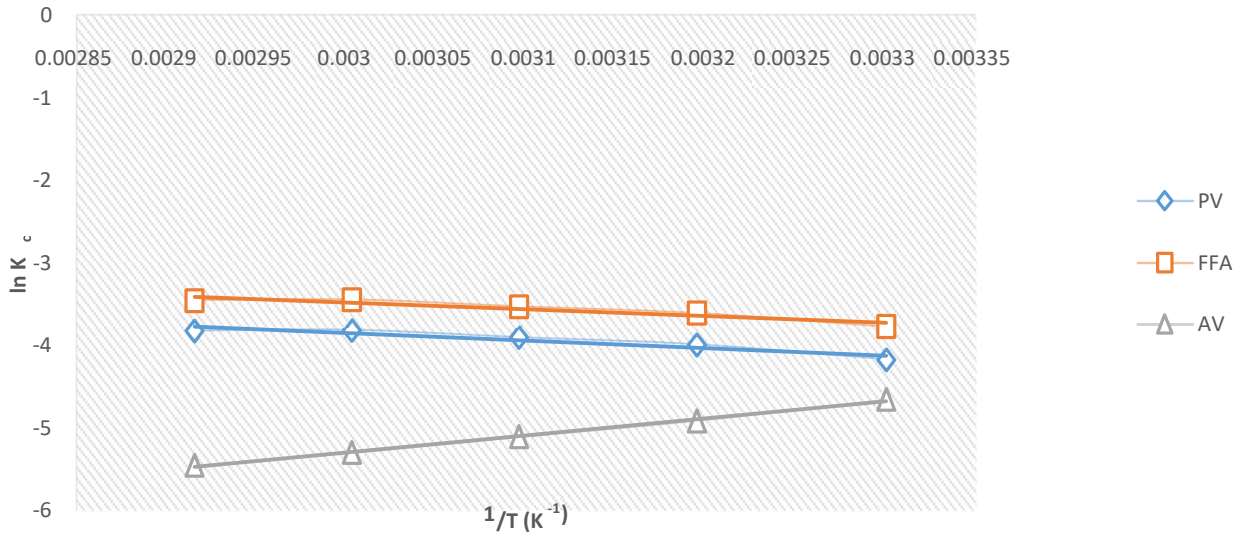

Figure 12. Adsorption thermodynamic plots of PO, FFA and ACD onto GSAC.

Table 4. Adsorption Thermodynamics of PO, FFA and ACD onto groundnut shell activated carbon

		Temperature				
Adsorbate_GSAC	Parameters	303	313	323	333	343
PO	ΔG	-4.78 x 10^3	-4.68 x 10^3	-4.59 x 10^3	-4.50 x 10^3	-4.40 x 10^3
	ΔH			7.59 x 10^4		
	ΔS			-9.28		
FFA	ΔG	-4.28 x 10^3	-4.19 x 10^3	-4.11 x 10^3	-4.02 x 10^3	-3.94 x 10^3
	ΔH			6.84 x 10^4		
	ΔS			-8.45		
ACD	ΔG	-4.61 x 10^4	-4.71 x 10^4	-4.8 x 10^4	-4.90 x 10^4	-4.99 x 10^4
	ΔH			1.72 x 10^4		
	ΔS			-95.55		

4. CONCLUSIONS

The GSAC possesses high fixed carbon content and surface areas together with well-developed pore structures. The presence of functional groups like OH, N-H, C-C, COOH boosts its good surface chemistry. The adsorption cycle was reliant upon dosage, contact time and temperature, and experimental data fittings exposed that Freundlich isotherm model fitted well for PO, FFA and ACD adsorption onto GSAC, while BWS, PSO and FPSO kinetic models respectively gave the goodness of fit. Adsorption thermodynamics revealed that the process was extemporaneous, endothermic and well-ordered.

Acknowledgments: The authors wish to thanks the management of Ladoke Akintola University of Technology Ogbomoso, Oyo State, Nigeria.

Conflict of interest: The authors declare that there is no conflict of interest.

References

[1] Babayemi A. K. (2017). Effects of Activating Chemicals on the Adsorption Capacity of Activated Carbons Prepared from Palm Kernel Shells. *Journal of Environmental Science, Toxicology and Food Technology*, 11(1), 60-64.

[2] Abdel-Shafy H. I., & Mansour, M. S. M. (2018). Solid waste issue: Sources, composition, disposal, recycling, and valorization: A review. *Egyptian Journal of Petroleum,* 27, 1275-1290.

[3] Loizides, M. I., Loizidou, X. I., Orthoxous, D. L., & Petsa, D. (2019). Circular bioeconomy in action: collection and recycling of domestic used cooking through a social reverse logistics system. *Recycling,* 4, 6-14.

[4] Ferronato, N., & Torretta, V. (2019). Waste mismanagement in developing countries: a review of global issues. *International Journal Environmental Resources and Public Health,* 16, 1060. https://doi.org/10.3390/ijerph16061060

[5] Biswas, S., Nandy, A., Islam N., & Rafa, N. (2020). Environmental citizenship and solid waste management in Chattegam, Banglandish: A review. *Open Economics.,* 3, 135-150. https://doi.org/10.1515/openec-2020-0109

[6] Pandit, A., Nakagawa, Y., Timilsina, R. R., Kotani, K., & Saijo, T. (2021). Taking the perspectives of future generations as an effective method for achieving sustainable waste management. *Sustainable Production and Consumption*, 27, 1526-1536.

[7] Kondoh, E., Edem, K. K., Bodjona, M.B., Kili, K. A., & Tchagbedji, G. (2021). Survey and quantification of household waste in Tsevie City, Togo. *Asian Journal of Chemistry,* 33(4), 802-806.

[8] Onawumi, O. O. E., Ibrahim, A.O., Opawale, R. O., & Akunola, A. A., & Ayoola, P. B. (2017). Purification of Used Frying Vegetable Oil using Eggshell and Maize Cob as Adsorbent. *Centrepoint Journal*, 23(1), 19-29.

[9] Boadu, K. O., Joel, O.F., Essumang, D. K., & Evbuomwan, B. (2018). Comparative Studies of the Physicochemical Properties and Heavy Metals Adsorption Capacity of Chemical Activated Carbon from Palm Kernel, Coconut and Groundnut Shells. *Journal of Applied Science Environmental. Management*, 22(1), 1833–1839.

[10] Ajala, L. O., & Ali, E. E. (2020). Preparation and Characterization of Groundnut Shell-Based Activated Charcoal. *Journal of Applied Sciences and Environmental. Management*, 24(12), 2139-2146.

[11] Abraham, F. A, Thenmozhi, R., Sivakumar, M., Sivakumar, K., Sasikuma, G., Thamaraimuthuayyanraj, S. (2018). Waste water treatment unit using activated charcoal. *International Resource. Journal of Engineering and Technology,* 5 (3), 312-315.

[12] Jacob, A. G., Okunola, O. J., Uduma, A. U., Tijjani, A., & Hamisu, S. (2017). Treatment of waste water by activated carbon developed from *Borassus aethiopum. Nigerian Journal of Material Science and Engineering,* 6 (1), 103-107.

[13] Prusty, J. K., & Patrol, S. K. (2015). Properties of fresh and hardened concrete using agro waste as partial replacement of coarse aggregate- a review. *Construction and Building Materials,* 82, 101-113.

[14] Oladoja, N. A., Adelagun, R. O. A., Ololade, I. A., Anthony, E. T., & Alfred, M. O. (2014). Synthesis of nano-sized hydrocalumite from a Gastropod shell for aqua system phosphate removal. *Separation and Purification Technology,* 124, 186-194.

[15] Ijaola, O. O., Ogedengbe, K., & Sangodoyin, A. Y. (2013). On the efficacy of activated carbon derived from bamboo in the adsorption of water contaminants. *International. Journal of Engineering Inventions*, 2(4), 29-34.

[16] Sivakumar, V., Asaithambi, M., & Sivakumar, P. (2012). Physic-chemical and adsorption studies of activated carbon from agricultural waste. *Journal of Engineering,* 5(5), 54-63.

[17] Ajayi-Banji, A., Sangodoyin, A., & Ijaola, O. (2015). Coconut husk Char Biosorptivity in Heavy Metal Diminution from Contaminated Surface Water. *Journal of Engineering Studies and Research,* 21(4), 7-13.

[18] Marichelvan, M. K., & Azhagurajan, A. (2018) Removal of mercury from effluent solution by using banana corm and neem leaves activated charcoal. *Environ. Nanotechnol. Monit. Manage,* 10, 360-365.

[19] Gokhale, N. A., Trivedi, N. S., Mandavgane, S. A., & Kulkarni, B. D. (2020). Biomass ashes as potent adsorbent for pesticide: prediction of adsorption by artificial neural network. *International Journal of Environmental Science and Technology,* 17, 3209-3216.

[20] Nandini, N., & Sivasakthivel, S. (2014). Bleaching of sunflower waste oil by adsorption on activated carbon and improved by ozonization. *American International Journal of Research in Science, Technology, Engineering and Mathematics,* **7** (1), 35-39.

[21] Wu, W., Zhang, X., Yang, J., Li, J., & Li, X. (2020). Facial preparation of oxygen-rich activated carbon from petroleum coke for enhancing methylene blue adsorption. *Carbon Letter,* 30, 627-636.

[22] Mansour, R. A., Shahawy, A. E., Attia, A., & Beheary, M. S. (2020). Brilliant green dye biosorption using activated carbon derived from guava tree wood. *International Journal of Chemical Engineering,* 2020, 1-12. https://doi.org/10.1155/2020/8053828

[23] Ani, J. U., Akpomie, K.G, Okoro, U.C., Aneke, L. E., Onukwuli, O.D., & Ujam, O. T. (2020). Potentials of activated carbon produced from biomass materials for sequestration of dyes, heavy metals and crude oil components from aqueous environment. *Applied Water Sci*ence, 10(69), 1-11.

[24] Mopoung, S., Moonsri, P., Palas, W., & Khumpai, S. (2015) Characterization and properties of activated carbon prepared from tamarind seeds by KOH activation for KOH activation for Fe (III) adsorption from aqueous solution. *The Science World Journal,* 2015: 1-9. http://dx.doi.org/10.1155/2015/415961

[25] Elelu, S., Adebayo, GB., Abduls-Salam, N., & Iriowen, E. M. (2019). Preparation and characterization of adsorbents from physic nut plant (*Jatropha curcas L*). *The Chemist,* 91 (2), 42-49.

[26] Didar, Z. (2017). Removal of impurities from waste oil using eggshell and its active carbon. *Journal Advanced Environmental and Health Resources,* 5, 123-130.

[27] Bello, O. S., & Ahmed, M. A. (2012). Coconut (*Cocosnucifera*) shell based activated carbon for the removal of malachite green dye from aqueous solutions. *Separation Science and Technology,* 46(6), 903-912.

[28] Saka, C. (2012). BET, TG-DTG, FT-IR, SEM, Iodine number analysis and preparation of activated carbon from acorn shell by chemical activation with Zn Cl_2. *Journal of Analytical and Applied Pyrolysis,* 95, 21-24.

[29] Ali, R. F. M., El & Anany, A. M. (2014). Recovery of used frying sunflower oil with sugar cane industry waste and hot water. *Journal Food Science Technology,* 51 (11), 3002-3013.

[30] Reza, M. S., Hasan, A.B.M., Afroze, K., Abu-Bakar, M. S., Taweekun, J., Azad, A. K. (2020). Analysis on preparation, application, and recycling of activated carbon to aid in Covid-19 protection. *International Journal of Integrated Engineering,* 12(5), 233-244.

[31] Gupta, V. K., Mittal, A., Mittal, J., Malviya, A., & Dipika., K. D. (2010). Decolorization treatment of hazardeous triarylmethane dye, Light Green SF (Yellowish) by waste material adsorbents. *Journal of Colloid Interdisciplinary Sciences,* 342(2), 518-527.

[32] Dawodu, M. O., Olutona, G. O., & Obimakinde, S. O. (2015). Effect of Temperature on the chemical characteristics of vegetable oils consumed in Ibadan, Nigeria. *Pakistan Journal of Nutrition,* 14(10), 698-707.

[33] Zhou, Y., Zhao, W., Lai, Y., Zhang, B., & Zhang, D. (2020). Edible Plant Oil: Global Status, Health Issues, and Perspectives. *Frontiers in Plant,* **11** (2020), 1315. https://doi.org/10.3389/fpls.2020.013115

[34] Zhang, D., Li, X., Zhang, Z., Zang, J., Sun, Q., Duan, X., Sun, H., & CaO, Y. (2022). Influence of roasting on the Physiochemical properties, Chemical composition and antioxidant activities of peanut oil. *Food Science and Technology,* 154 (2022), 112613. https://doi/10.1016/j.iwt.2021.112613

[35] Bavaresco, A., Fonseca, J.M., da Silva, C., & Teleken, J. G. (2021). Use of carbonized corn cob biomass to reduce acidity of residual frying oil. *Acta Scientiarum Technology,* 43, 51303. https://doi.org/10.4025/actascitechnol. v3i1.e51303

[36] Nurulain, S., Aziz, N. A., Salim, M. R., & Manap, H. (2021). A review of free fatty acid determination methods for palm cooking oil. *Journal of Physics: Conference Series,* 1921, 012055. https://doi.org/10.1088/1742-6596/1921/1/012055

[37] Ushedo, T. R., Adeyemi., O. G., Adewuyi, A., & Lau, W. (2022). Synthesis of N, N(1,3Phenylene) dimethanimine. A useful resource for the removal of free fatty acid in waste vegetable oil. *Scientific African,* 16, 01188. https://doi.org/10.1016/j.sciaf.2022.e01188

[38] Pal, U. S., Patra, R. K., Sahoo, N. R., Bakhara, C. K., & Panda, M. K. (2015). Effect of refining on quality and composition of sunflower oil. *Journal of Food Science and Technology,* 52, 4613-46-18.

[39] Ogori, A. F. (2020). Sources, Extraction and Constituents of fats and oils. *HSOA Journal of Food Science and Nutrition,* **6** (2), 1-8.

[40] [40] Unuabonah, E. I., Agunbiade, F. O., Alfred, M. O., Adewumi, T. A., Okoli, C. P., Omorogie, M. O., Akanbi, M. O., Ofomaja, A. E., & Taubert, A. (2017). Facile synthesis of new aminofunctionalized agrogenic hybrid Composite Clay adsorbents for phosphate capture and recovery from water. *Journal of Cleaner Production,* 164, 652-663.

[41] Olafadehan, O. A., Bello, V. E., Amoo, K. O., & Bello, A. M. (2022). Isotherms, kinetic and thermodynamic studies of methylene blue adsorption on chitosan flake derived from African giant snail shell. *African Journal of Environmental Science and Technology,* 16 (1), 37-70.

[42] Ebelegi, A. N., Toneth, E. I., & Bokizibe, M. A. (2022). Determination of Physiochemical Properties of Biosorbnts Synthesized from Water Melonb Rind Using Microwave Assisted Irradiation Procedure, *Open Journal of Physical Chemistry,* 12, 19-30.

[43] Nandiyanto, A. B. D., Oktiani, R., & Ragadhita, R. (2019). How to Read and Interpret FTIR Spectroscope of Organic Material. *Indonesian Journal of Science and Technology,* 4(1), 97118.

[44] Adeleke, A. E., Onifade, A. P., Jabar, J. M., & Sangoremi, A. A. (2023). Adsorption of Pb^{2+} from Simulated Solution using Raw Kola Nut Pod Adsorbent. *Nano Trends,* 25(1), 38-49.

[45] Jabar, J. M., Odusote, Y. A., Ayinde, Y. T., & Yilmaz, M. (2022). African almond (*Terminalia catappah*) leaves biochar prepared through pyrolysis using H_3PO_4 as chemical activation for sequestration of methylene blue dye. *Results in Engineering,* 14(2022), 100385. https://doi.org/101016/j.rineng.2022.100385